Microgravity Generation Using Tilting Board
for Resolution Evaluation of MEMS Accelerometer

Motohiro Takayasu,[1*] Ippei Tsuji,[1] Hiroyuki Ito,[1] Daisuke Yamane,[1] Shiro Dosho,[1]
Toshifumi Konishi,[1,2] Noboru Ishihara,[1] Katsuyuki Machida,[1] and Kazuya Masu[1]

[1]Tokyo Institute of Technology, Yokohama, Kanagawa 226-8503, Japan
[2]NTT Advanced Technology Corporation, Atsugi, Kanagawa 243-0124, Japan

We describe microgravity generation and the resolution evaluation results of a sub-1-mG microelectromechanical system (MEMS) accelerometer (1 G = 9.8 m/s^2). To realize input acceleration below 1 mG, we show the principle of generating microgravity acceleration by adjusting the tilt angle. The change in acceleration induced by a tilting board is quantitatively analyzed, and the capacitance change of the MEMS accelerometer as a function of tilt angle is measured. The analytical results show that the tilting board has the potential to generate microgravity. The experimental results reveal that the sub-1-mG MEMS accelerometer can realize the detection of sub-1-mG-level acceleration.

1. Introduction

Microelectromechanical system (MEMS) accelerometers have been widely used in various applications such as shock detection of vehicles, active stabilization of mobile robots, and motion detection of head-mounted displays.[1–4] High-resolution MEMS accelerometers could realize potential applications such as inertial navigation, earthquake prediction, and satellite control.[5–7] Thus, our group has developed MEMS accelerometers with sensing resolutions higher than 1 G (1 G = 9.8 m/s^2).[8–10]

The performance of MEMS accelerometers is affected by noise, including the Brownian noise B_n.[11–14] In practical use, the sensing resolution of MEMS accelerometers is evaluated using vibration exciters. As a result, accelerometer evaluation depends on the performance of vibration exciters.[15–18] There have been no vibration exciters generating microgravity acceleration because mechanical and electrical noises generate acceleration noise that is larger than microgravity. Thus, MEMS accelerometers have not been measured within a range of 10^2 mG. To investigate the characteristics of MEMS accelerometers at the input acceleration of sub-1 mG, we need a method of generating microgravity acceleration.

To realize input acceleration below 1 mG, we have investigated a method using a tilting board. By adjusting the tilt angles of the tilting board, this method would generate microgravity

acceleration. Although methods with rotation motors have been used in practice for the evaluation of MEMS inclinometers,[19–22] microgravity acceleration cannot be applied to such methods; thus, we have developed a MEMS inclinometer fabricated with the multilayer-metal technology[23] and a tilting-board method to evaluate the MEMS inclinometer.[24]

In this study, we investigated the possibility of generating microgravity acceleration and evaluating the sensing resolution of the developed sub-1-mG MEMS accelerometer[8–10] by the tilting-board method. First, we describe the approach for generating microgravity acceleration using a tilting board. Next, the inertial force applied to the MEMS accelerometer set on the tilting board is analytically obtained. Finally, we present the static characteristics of the sub-1-mG MEMS accelerometer determined by the tilting-board method.

2.   Principle

2.1   Microgravity generation

We show the principle of generating microgravity acceleration by adjusting the tilt angle. When the MEMS accelerometer is tilted by θ_x, the gravitational acceleration g (g = 1 G) is divided into acceleration along the sensing axis A_x and acceleration along the y-axis A_y, as shown in Fig. 1. A_x is defined as

$$A_x = \mathrm{g}\cos\theta_x \text{ [G]}. \tag{1}$$

The acceleration change A_{0x} is described by

$$A_{0x} = \mathrm{g} - \mathrm{g}\cos\theta_x \text{ [G]}. \tag{2}$$

Figure 2 shows the analytical result of A_{0x} as a function of θ_x. In Fig. 2(a), A_{0x} changes from 0 to 1 G, when θ_x changes from 0 to 90°. If θ_x is 0.10°, A_{0x} is 1.5 µG, as shown in Fig. 2(b). These results suggest that microgravity acceleration can be generated by adjusting θ_x.
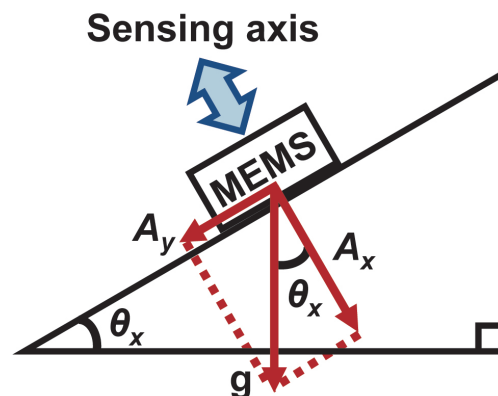

Fig. 1.   (Color online) Analytical modeling of inertial force acting on a MEMS accelerometer set on a tilting board.
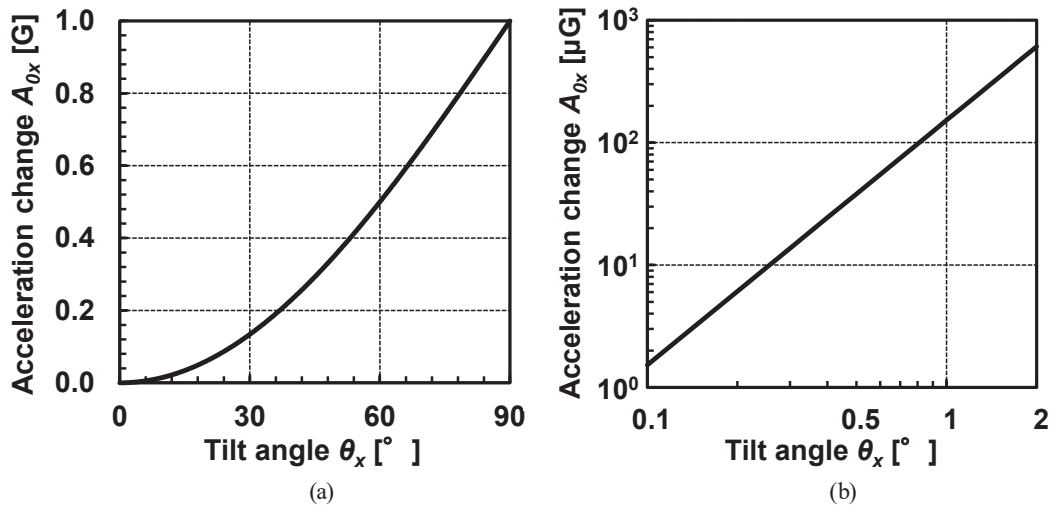
Fig. 2.   Analysis results of acceleration change as a function of tilt angle in the ranges (a) from 0 to 180° and (b) from 0.1 to 2°.
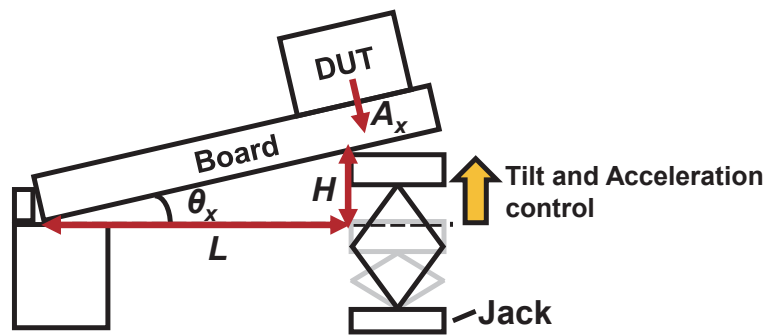

Fig. 3.   (Color online) Tilting-board method.

To generate microgravity acceleration by the above-mentioned principle, an evaluation apparatus is constructed.   Figure 3 shows the tilting-board method for sub-1-mG MEMS accelerometers.   The MEMS accelerometer is set on the tilting board.   The tilting board is composed of a jack and a board.   The tilt angle θ_x of the tilting board can be controlled by changing the height H of the jack. θ_x can be calculated from the distance L and H.

$$\theta_x = \tan^{-1}\left(\frac{H}{L}\right) [°] \tag{3}$$

When Eq. (3) is substituted into Eq. (2), A_{0x} is described by

$$A_{0x} = g - g\cos\left\{\tan^{-1}\left(\frac{H}{L}\right)\right\} [G]. \tag{4}$$
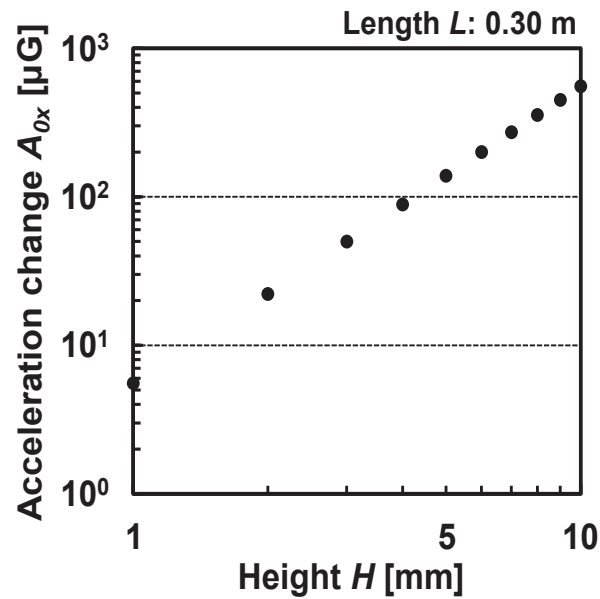
Fig. 4.   Analysis results of acceleration change as a function of tilting-board height.
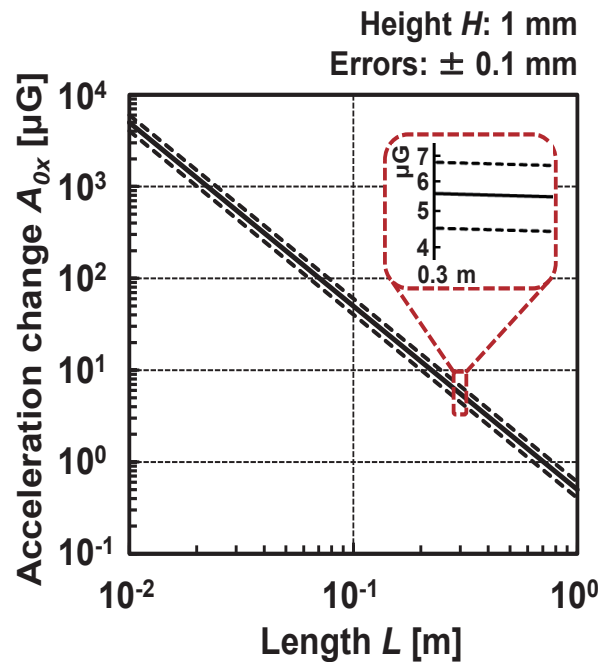

Fig. 5.   (Color online) Analysis results of acceleration change as a function of tilting-board length.

In Fig. 4, L is set to be 0.30 m and H is changed in 1 mm steps; thereby, we can realize A_{0x} with a sub-1-mG resolution.   The longer the L we set, the smaller A_{0x} becomes, as shown in Fig. 5.   When L is set to be 1 m and H is changed from 0 to 1 mm with an error of ±0.1 mm, A_{0x} becomes 0.5 ± 0.1 µG.   By this method, we could apply microgravity acceleration to the MEMS accelerometer and analyzed the capacitance change of the sub-1-mG MEMS accelerometer as a function of microgravity acceleration.

2.2   Detection of acceleration

A schematic model of the sub-1-mG MEMS capacitive accelerometer is shown in Fig. 6.[8–10] When acceleration is applied to the MEMS accelerometer, C_s is changed. C_p is capacitance in the SiO$_2$ film. The total capacitance C_x of the MEMS accelerometer on the tilting board shown in Fig. 1 is defined by

$$C_x = \varepsilon_0 \frac{S}{d' - \dfrac{9.8mg\cos\theta_x}{k}} \ [\text{F}],$$

(5)

where ε_0, S, and k are the dielectric constant of vacuum, the proof-mass area, and the spring constant, respectively. d' is described by

$$d' = d_0 + \frac{d_1}{\varepsilon_2} \ [\text{m}],$$

(6)

where d_0, d_1, and ε_2 are the initial gap between the proof mass and the SiO$_2$ film, the thickness of the SiO$_2$ film, and the dielectric constant of SiO$_2$, respectively. When θ_x is 0°, the capacitance C_0 of the MEMS accelerometer is determined by

$$C_0 = \varepsilon_0 \frac{S}{d' - \dfrac{9.8mg}{k}} \ [\text{F}].$$

(7)

Thus, the capacitance change C_{0x} of the MEMS accelerometer is analytically obtained by

$$C_{0x} = C_0 - C_x = \varepsilon_0 \frac{S}{d' - \dfrac{9.8mg}{k}} - \varepsilon_0 \frac{S}{d' - \dfrac{9.8mg\cos\theta_x}{k}} \ [\text{F}].$$
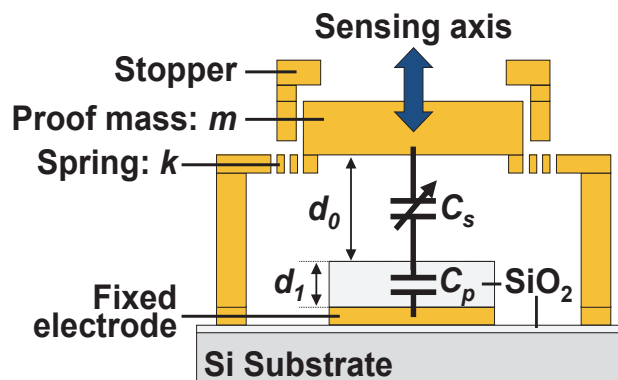
(8)

Fig. 6.   (Color online) Schematic model of the sub-1-mG MEMS capacitive accelerometer.[8–10]

3.   Experimental Results

To experimentally confirm the above principles, the MEMS accelerometer was fabricated by gold electroplating, as shown in Fig. 7(a).[8–10] The proof-mass area was designed to be 2.0×2.0 mm^2. Each corner of the proof-mass was suspended by micromechanical suspension. A sensor module was composed of the MEMS accelerometer and a capacitance-to-digital converter (CDC; AD7745, Analog Devices), as shown in Fig. 7(b). The capacitance change of the MEMS accelerometer was obtained using the CDC. The microcontroller (Arduino Due, Arduino) received digital signals from the CDC and sent them to a personal computer (PC) to store the data.

To evaluate the sensing resolution of the MEMS accelerometer, the frequency response of the MEMS accelerometer was measured using the LCR meter (HIOKI E.E. IM3533-01). Figure 8 shows the capacitance and phase changes as a function of the sensing-signal frequency. The mechanical resonant frequency f_{res} and quality factor Q were measured to be 445 Hz and 3.29, respectively. By using the results,[9] the actual B_n was estimated to be 398 nG/√Hz, as summarized in Table 1. These results confirm that the sub-1-mG MEMS accelerometer has the capability to detect acceleration below 1 mG.
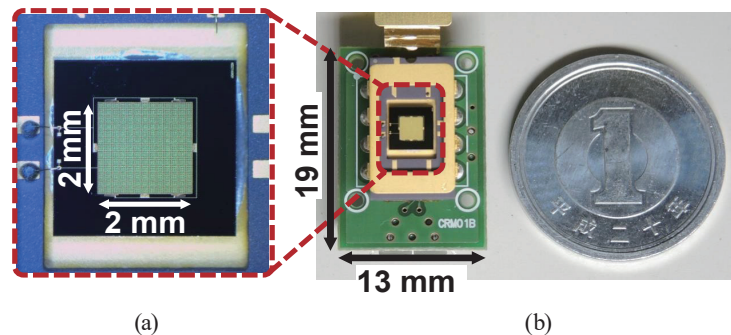

Fig. 7.   (Color online) Photographs of (a) MEMS accelerometer and (b) sensor module.
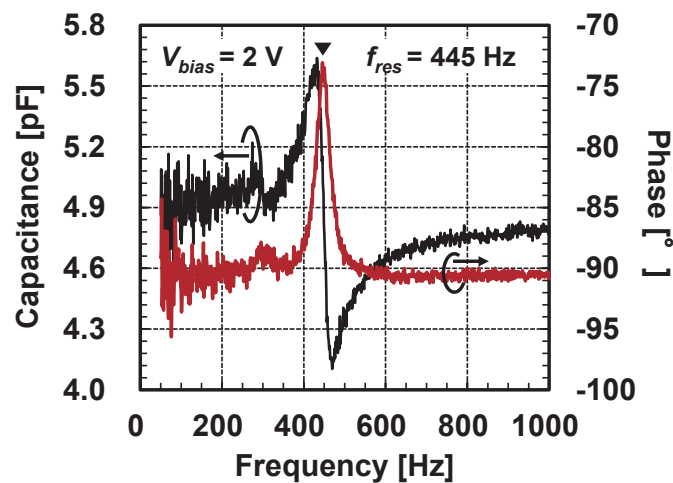

Fig. 8.   (Color online) Measured capacitance and phase as a function of sensing-signal frequency.

Table 1
Design and measured parameters of the MEMS accelerometer.

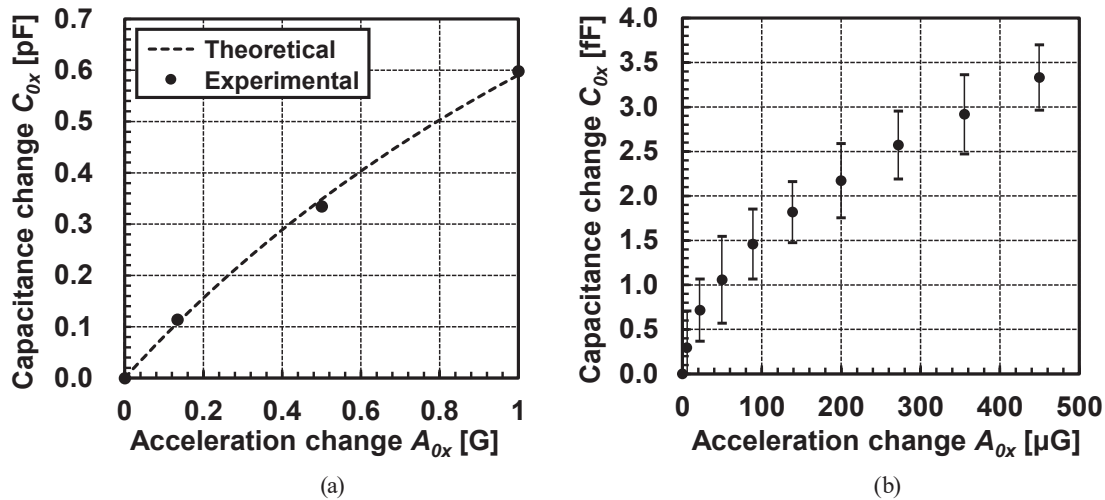| Parameters	Design	Measured	Unit
m	8.43×10^{-7}	9.27×10^{-7}	kg
f_{res}	262	445	Hz
Q	3.00×10^{-1}	3.29	—
B_n	67.0	398	nG/√Hz

Fig. 9.   Measured capacitance change as a function of acceleration change ranging (a) from 0 to 1 G and (b) from 0 to 500 µG.

The microgravity characteristics of the MEMS accelerometer were evaluated by the tilting-board method. The sensor module was set on a tilting board, where L was set to be 0.30 m. A_{0x} was calculated using Eq. (4) and measured using the reference tilt sensor (BBMO-66, MonotaRO). Figure 9(a) shows C_{0x} as a function of A_{0x} ranging from 0 to 1 G. The plotted points in Fig. 9(a) are the averaged experimental results of C_{0x}, and the dashed line is the fitting curve derived using Eq. (8) with parasitic capacitances. These results indicate that the MEMS accelerometer could measure microgravity acceleration; the experimental results coincide with the theoretical model. Figure 9(b) shows the measured C_{0x} as a function of A_{0x} ranging from 0 to 500 µG. The plotted points in Fig. 9(b) are the average values, and the error bars show the maximum and minimum values. The results indicate that the sensor module has a potential to detect microgravity acceleration below 100 µG. By applying actual microgravity acceleration by the tilting-board method, we confirmed that the sub-1-mG MEMS accelerometer had the capability to detect microgravity acceleration with a sensing resolution higher than 100 µG.

4.   Conclusions

We discussed the microgravity generation and resolution evaluation results of the sub-1-mG MEMS accelerometer. To realize input acceleration below 1 mG, we showed the principle of generating microgravity acceleration by adjusting the tilt angle. The acceleration changes

obtained with the tilting board were quantitatively analyzed, and capacitance changes of the MEMS accelerometer as a function of tilt angle were measured. The analytical results showed that the tilting board had the capability to generate microgravity. The experimental results revealed that the sub-1-mG MEMS accelerometer could realize the detection of sub-1-mG-level acceleration.

Acknowledgments

References

1   B. E. Boser and R. T. Howe: IEEE J. Solid-State Circuits **31** (1996) 366.
2   N. Yazdi, F. Ayazi, and K. Najafi: Proc. IEEE **86** (1998) 1640.
3   N. Barbour and G. Schmidt: IEEE Sens. J. **1** (2001) 332.
4   C. Acar and A. M. Shkel: J. Micromech. Microeng. **13** (2003) 634.
5   B. V. Amini and F. Ayazi: J. Micromech. Microeng. **15** (2005) 2113.
6   G. Krishnan, C. U. Kshirsagar, G. K. Ananthasuresh, and N. Bhat: J. Indian Inst. Sci. **87** (2007) 333.
7   J. Wu, G. K. Fedder, and L. R. Carley: IEEE J. Solid-State Circuits **39** (2004) 722.
8   K. Machida, T. Konishi, D. Yamane, H. Toshiyoshi, and K. Masu: ECS Trans. **61** (2014) 6.
9   D. Yamane, T. Konishi, T. Matsushima, K. Machida, H. Toshiyoshi, and K. Masu: Appl. Phys. Lett. **104** (2014) 074102.
10   D. Yamane, T. Konishi, H. Toshiyoshi, K. Masu, and K. Machida: ECS Trans. **72** (2016) 7.
11   T. B. Gabrielson: IEEE T. Electron Dev. **40** (1993) 903.
12   J. Wu, G. K. Fedder, and L. R. Carley: IEEE J. Solid-State Circuits **39** (2004) 722.
13   H. Sun, D. Fang, K. Jia, F. Maarouf, H. Qu, and H. Xie: IEEE Sens. J. **11** (2011) 925.
14   M. H. Tsai, Y. C. Liu, and W. Fang: J. Microelectromech. Syst. **21** (2012) 1329.
15   M. Lemkin and B. E. Boser: IEEE J. Solid-State Circuits **34** (1999) 456.
16   H. Kulah, J. Chae, N. Yazdi, and K. Najafi: IEEE J. Solid-State Circuits **41** (2006) 352.
17   T. Konishi, D. Yamane, T. Matsushima, G. Motohashi, K. Kagaya, H. Ito, N. Ishihara, H. Toshiyoshi, K. Machida, and K. Masu: Jpn. J. Appl. Phys. **52** (2013) 06GL04.
18   H. Xu, X. Liu, and L. Yin: IEEE J. Solid-State Circuits **50** (2015) 2101.
19   S. Luczak and W. Oleksiuk: Eng. Mech. **14** (2007) 143.
20   S. S. Yun, D. H. Jeong, S. M. Wang, C. H. Je, M. L. Lee, G. Hwang, C. A. Choi, and J. H. Lee: J. Micromech. Microeng. **19** (2009) 035025.
21   S. Luczak: Eng. Mech. **18** (2011) 341.
22   F. S. Alves, R. A. Dias, J. M. Cabral, J. Gaspar, and L. A. Rocha: J. Microelectromech. Syst. **24** (2015) 931.
23   K. Machida, S. Shigematsu, H. Morimura, Y. Tanabe, N. Sato, N. Shimoyama, T. Kumazaki, K. Kudou, M. Yano, and H. Kyuragi: IEEE Trans. Electron Devices. **48** (2001) 2273.
24   I. Tsuji, M. Takayasu, H. Ito, D. Yamane, S. Dosho, T. Konishi, N. Ishihara, K. Machida, and K. Masu: Proc. 2017 Int. Conf. Solid-State Devices and Materials (SSDM, 2017) 369.